

First-principles study of $(\text{BiScO}_3)_{1-x}-(\text{PbTiO}_3)_x$ piezoelectric alloys

Jorge Íñiguez,¹ David Vanderbilt,¹ and L. Bellaiche²

¹*Department of Physics and Astronomy, Rutgers University, Piscataway, New Jersey 08854-8019, USA*

²*Physics Department, University of Arkansas, Fayetteville, Arkansas 72701, USA*

(January 31, 2003)

We report a first-principles study of a class of $(\text{BiScO}_3)_{1-x}-(\text{PbTiO}_3)_x$ (BS-PT) alloys recently proposed by Eitel *et al.* as promising materials for piezoelectric actuator applications. We show that (i) BS-PT displays very large structural distortions and polarizations at the morphotropic phase boundary (MPB) (we obtain a c/a of ~ 1.05 - 1.08 and $P_{\text{tet}} \approx 0.9$ C/m²); (ii) the ferroelectric and piezoelectric properties of BS-PT are dominated by the onset of hybridization between Bi/Pb- $6p$ and O- $2p$ orbitals, a mechanism that is enhanced upon substitution of Pb by Bi; and (iii) the piezoelectric responses of BS-PT and $\text{Pb}(\text{Zr}_{1-x}\text{Ti}_x)\text{O}_3$ (PZT) at the MPB are comparable, at least as far as the computed values of the piezoelectric coefficient d_{15} are concerned. While our results are generally consistent with experiment, they also suggest that certain intrinsic properties of BS-PT may be even better than has been indicated by experiments to date. We also discuss results for PZT that demonstrate the prominent role played by Pb displacements in its piezoelectric properties.

I. INTRODUCTION

Perovskite alloys based on PbTiO_3 (PT) are of considerable interest for applications as piezoelectric actuator materials.^{1,2} The phase diagrams of the most technologically important alloys are characterized by a morphotropic phase boundary (MPB) separating the PT-rich tetragonal phase, in which the polarization lies along a $\langle 001 \rangle$ direction, from the PT-poor rhombohedral phase, in which the polarization is along a $\langle 111 \rangle$ direction.³ Because the structural transition between these two phases brings about a large electromechanical response, materials with a composition lying close to the MPB are the preferred ones for applications. Examples of such materials are PZT or PZN-PT, in which PT is alloyed with PbZrO_3 (PZ) or $\text{Pb}(\text{Zn}_{1/3}\text{Nb}_{2/3})\text{O}_3$, respectively.

Recently, attention has been drawn to a new class of materials in which PT is alloyed with Bi-based perovskites, the best-studied example being $(\text{BiScO}_3)_{1-x}-(\text{PbTiO}_3)_x$ (BS-PT).⁴ The appeal of BS-PT is twofold: (i) it appears to have piezoelectric properties comparable to those of PZT and PZN-PT in quality, and (ii) its dielectric and piezoelectric properties should be more robust, over a wider temperature range, than those of PZT and PZN-PT. The physical reason behind (ii) is that the Curie temperature within the MPB composition range (T_C^{MPB}) is higher in BS-PT ($\sim 450^\circ\text{C}$) than in PZT ($\sim 400^\circ\text{C}$) or PZN-PT ($\sim 200^\circ\text{C}$), suggesting that BS-PT at room temperature will age more slowly, its properties will be more temperature-independent, etc.^{2,4} A possible drawback is that BS-PT is evidently not thermodynamically stable in the perovskite crystal structure over the entire range of composition. However, for applications purposes it is only important that the perovskite structure can be obtained for compositions near the MPB, and this is indeed the case.

The authors of Ref. 4 synthesized BS-PT guided by an empirical crystal-chemistry rule suggesting that since

Bi^{3+} is too small an ion to form a cubic perovskite with Sc^{3+} , it will have a strong tendency to move off-center from its high-symmetry position, yielding a high structural transition temperature. While perhaps overly simplistic, this reasoning is undoubtedly partially correct and is likely to be useful for materials engineering. However, it is unclear how to explain the large piezoelectric responses found in BS-PT based on ion-size considerations alone. The ferroelectric properties of materials like PZT are known to be related to the partial covalency of some bonds,^{5,6} and the situation in BS-PT should be similar. On the other hand, most of the relevant piezoelectric alloys have only Pb on the A site of their perovskite structure, and the chemistry of Pb is known to be very important to their properties.⁷ The substitution of Pb by Bi in BS-PT is thus of particular interest in view of the good piezoelectric properties of this material.

We present here a first-principles study of BS-PT. We find that Bi plays a crucial role, and in particular that hybridization between Bi- $6p$ and O- $2p$ orbitals is the driving force for the ferroelectric instabilities of BS-PT, allowing for very large polarizations and responses. Our results are generally consistent with experiment, but they also suggest that the intrinsic ferroelectric and piezoelectric properties of BS-PT alloys might be even better than those measured experimentally to date.

We present our results in the form of a systematic comparison of the properties of BS-PT with those of PZT. Section II describes the first-principles methods employed. In Sec. III we study the ferroelectric instabilities of pure BS, PT, and PZ, introducing some corresponding calculations on BiYO_3 (BY) as an aid to the discussion. In Sec. IV we discuss the ferroelectric instabilities of the alloys and make contact with the experimental results, while Sec. V is devoted to the piezoelectric properties of the alloys near the MPB. We summarize and conclude in Sec. VI.

TABLE I. Relaxed structure and polarization for BiScO₃ (BS), PbTiO₃ (PT), PbZrO₃ (PZ), BiYO₃ (BY), a VCA BS-PT alloy at $x = 0.5$ (BS-PT (VCA)), a 10-atom BS-PT supercell (BS-PT (SC)), a VCA PZT alloy at $x = 0.5$ (PZT (VCA)), and a 10-atom PZT supercell (PZT (SC)). (See text for details.) Reported are the tolerance factor t ; the energy difference ΔE (in eV) per 5-atom cell relative to the cubic phase, and the polarization P (in C/m²), for tetragonal and rhombohedral phases; and the c/a ratio and the rhombohedral angle α (in degrees) for the tetragonal and rhombohedral phases respectively. BS-PT (SC) has two inequivalent rhombohedral phases; the reported results correspond to the lower-energy phase.

System	t	Tetragonal phase			Rhombohedral phase		
		ΔE	c/a	P	ΔE	α	P
BS	0.907	-1.124	1.285	0.93	-1.353	88.6	0.47
PT	1.027	-0.060	1.049	0.82	-0.047	89.6	0.72
PZ	0.970	-0.214	1.035	0.73	-0.274	89.5	0.78
BY	0.845	-2.260	1.376	0.95	-2.896	88.7	0.49
BS-PT (VCA)		-0.376	1.114	0.92	-0.412	89.1	0.60
BS-PT (SC)		-0.472	1.079	1.06	-0.565	89.4	1.05
PZT (VCA)		-0.060	1.026	0.69	-0.061	89.6	0.67
PZT (SC)		-0.096	1.032	0.73	-0.104	89.5	0.72

II. METHODS

The calculations were performed within a plane-wave implementation of the local-density approximation (LDA) to density-functional theory, using ultrasoft pseudopotentials⁸ to represent the ionic cores. The following electronic states were included in the calculation: the $2s$ and $2p$ states of O, the $3s$, $3p$, $3d$, and $4s$ states of Sc and Ti, the $4s$, $4p$, $4d$, and $5s$ states of Y and Zr, and the $5d$, $6s$, and $6p$ states of Pb and Bi. For the 5-atom unit cell calculations, we used a 35 Ry plane-wave cutoff and a $6 \times 6 \times 6$ k-point grid for Brillouin zone integrations. We checked that these choices yield converged results. We also made some calculations with a rocksalt-ordered (fcc) 10-atom unit cell, for which we used a 30 Ry cutoff and a $4 \times 4 \times 4$ k-point grid. Atomic relaxations were considered to be converged when the residual forces were smaller than 5×10^{-5} a.u. Polarizations were computed using the Berry-phase expression of King-Smith and Vanderbilt⁹ and always using a dense-enough k-point mesh along the direction of the strings. The character of the electron energy bands was estimated by computing the partial density associated with the pseudopotential projectors of specific atoms (see Eq. (19) of Ref. 8 for guidance).

Calculations using the virtual-crystal approximation (VCA) were implemented as in Ref. 10. In the VCA one works with virtual atoms defined by a pseudopotential that is a weighted average of those of real atoms. Such a procedure may lead to meaningful estimates of the average properties of an alloy provided that the valence orbitals of the real atoms forming the virtual atom are similar in character. This can be expected to be true for the pairs Bi-Pb and Sc-Ti in BS-PT. Also, both groups BiSc and PbTi have a total nominal ionic charge of +6, allowing them to be mixed in arbitrary proportions. These requirements are also satisfied by PZT, which has previously been studied within the VCA.^{10,11} It is important to note that the VCA is not expected to render an ac-

curate description of the electronic structure of a truly disordered alloy, but rather to provide us with qualitative energetic and structural trends. Also, the VCA is expected to work better for isovalent pairs of atoms (e.g., Zr-Ti) than for heterovalent pairs (e.g., Bi-Pb or Sc-Ti), which makes BS-PT a particularly challenging system. For this reason, we assess the reliability of our VCA results by comparing them with some supercell calculations and available experimental information.

III. PURE COMPOUNDS

As a preliminary step towards understanding BS-PT, we first consider pure BS (in the perovskite structure¹²) and compare with corresponding calculations for pure PT and PZ. The first three lines of Table I show the structural and polarization results obtained by relaxing these systems within ferroelectric phases of tetragonal ($P4mm$) or rhombohedral ($R3m$) symmetry, always maintaining a 5-atom unit cell. The atomic relaxations corresponding to the tetragonal phases of BS and PT are given in Table II.

For BS, we find the rhombohedral phase to be lower in energy than the tetragonal phase, which agrees with the

TABLE II. Lattice constant c and atomic coordinates (relative to A site, in units of c) in the tetragonal phase of several systems (following the notation of Table I). Note that the ideal cubic-perovskite coordinates are $z(\text{B})=0.5$, $z(\text{O}_x, \text{O}_y)=0.5$, and $z(\text{O}_z)=0.0$.

	BS	PT	BY	(VCA)	(VCA)
				BS-PT	PZT
c (a.u.)	9.14	7.65	10.00	8.07	7.65
$z(\text{B})$	0.573	0.535	0.575	0.571	0.547
$z(\text{O}_x, \text{O}_y)$	0.729	0.606	0.761	0.682	0.610
$z(\text{O}_z)$	0.177	0.094	0.180	0.145	0.085

experimental fact that BS-rich BS-PT is rhombohedral, and we find that the relaxations are very large. This is reflected both in the structural data (we obtain $c/a = 1.29$ for the tetragonal phase of BS, compared with 1.05 for PT; see also the atomic displacements in Table II) and in the energetics (ΔE_{tet} and ΔE_{rho} of BS are one order of magnitude larger than for PT and PZ). These results suggest that the cubic perovskite structure is not a very natural one for BS, a conclusion which is reinforced by experimental indications that pure BS at zero pressure is not even thermodynamically stable.⁴

The polarization associated with the tetragonal phase of BS is large,¹³ while that of the rhombohedral phase is relatively small. In both cases, the largest contribution to P comes from the displacement of Bi relative to its neighboring O ions (O_x and O_y in Table II). More specifically, in the cubic phase of BS all effective charges are normal, i.e., with values close to the nominal ionic charges, except for those of Bi (6.4) and O_x and O_y (-3.2 along the polarization direction). Moreover, these are the ions with the largest relative displacements associated with the ferroelectric instability (see Table II). The difference in P between the two phases reflects a significantly smaller charge transfer when the Bi ion approaches three O ions (rhombohedral phase) instead of four (tetragonal phase).

The fundamental role of Bi in the ferroelectric instabilities of BS is best appreciated in the electronic band-structure data shown in Fig. 1. As in PT (panel c), the top valence states of the cubic phase of BS (panel a) are O-2p in character. However, the lowest unoccupied states of BS are Bi-6p like, at variance with the Ti-3d bands we find in PT. This fact, together with the relatively small gap of cubic BS, results in ferroelectric instabilities mainly characterized by a hybridization between Bi-6p and O-2p orbitals, not the one involving d bands of the B cation that is typical of most other ferroelectric perovskites.^{6,14,15} In the tetragonal phase of BS (panel b), the gap opens considerably and the top valence bands increase their Bi-6p character. The strong Bi-6p–O-2p hybridization is also reflected in the fact that the effective charge of Bi in the tetragonal phase recovers a normal value (2.9 along the polarization direction).

As indicated earlier, Eitel and co-workers chose to study BS-PT because of the large size mismatch between Bi and Sc.⁴ Such a mismatch is conveniently quantified in terms of the tolerance factor

$$t = \frac{R_A + R_O}{\sqrt{2}(R_B + R_O)}, \quad (1)$$

where R_O , R_A and R_B are the ionic radii of oxygen and of the A and B cations respectively.¹⁶ That is, t is the ratio between the ideal cubic lattice parameters based on A–O vs. B–O bonding alone, with $t=1$ corresponding to high perovskite stability. As can be seen from Table I, the relatively low value of $t=0.907$ for BS implies that the Bi ion should be very unstable in the high-symmetry position of the cubic perovskite structure, consistent with

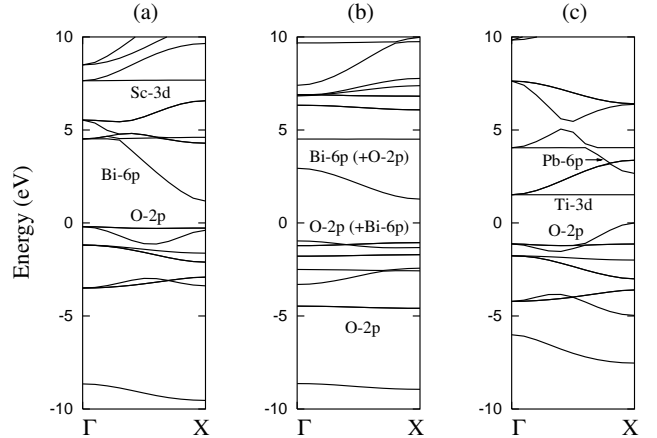


FIG. 1. Near-gap electronic band structure along the Γ -X direction for (a) cubic BS, (b) tetragonal BS, and (c) cubic PT. Zero of energy is at the valence-band maximum.

our findings. We also studied BiYO₃ (BY), for which $t=0.845$, and found even stronger ferroelectric instabilities that are very similar in character to those of BS (see Tables I and II). However, P_{tet} and P_{rho} of BY are almost identical to those of BS, not larger. Also, the distance between Bi and its bonded O neighbors is roughly the same in the ferroelectric phases of BS and BY (4.33 and 4.35 a.u., respectively, in the tetragonal phase). These two facts seem to indicate that the onset of the Bi-6p–O-2p hybridization (which also dominates the development of polarization in BY) is not very t -dependent, suggesting that the large polarizations of BS and BY cannot be attributed mainly to a size-mismatch effect. Instead, they are strongly linked to the particular chemistry of Bi, i.e., its strong tendency to bond covalently with the surrounding oxygen anions.

IV. ALLOYS: FERROELECTRIC INSTABILITIES

We now turn to a study of the BS-PT alloy within the virtual crystal approximation (VCA).^{10,11} We also carry out parallel VCA calculations on the PZT alloy as a relevant reference.

Figure 2 shows the energies of the tetragonal and rhombohedral ferroelectric phases of BS-PT and PZT. (The cubic phase, which is material- and composition-dependent, is chosen as the zero of energy.) Structural and polarization results corresponding to those obtained for the pure compounds are shown in Tables I and II.

Associating the MPB composition with the crossing of the energy curves for the two ferroelectric phases in Fig. 2, we estimate $x_{\text{MPB}} \approx 0.65$ for BS-PT, while the experimental value is 0.64.⁴ Similarly, for PZT we get $x_{\text{MPB}} \approx 0.55$, to be compared with experimental values from about 0.45 to about 0.52 (the range of stability

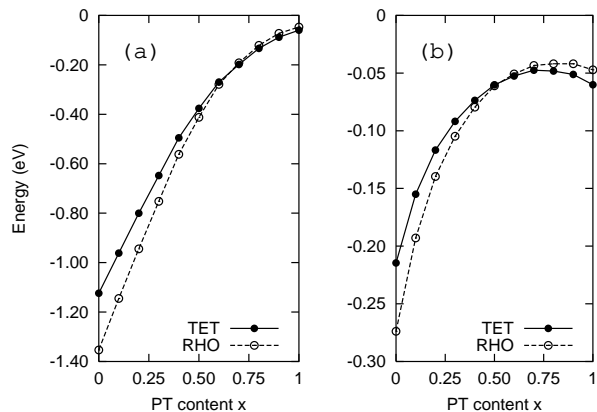


FIG. 2. Calculated VCA energies of the tetragonal and rhombohedral phases, relative to the cubic phase, as a function of PT content for BS-PT (panel a) and PZT (panel b). Note the two different energy scales.

of the intermediate monoclinic phase of PZT³). Taking into account all the approximations involved in our estimation, we must regard the agreement in the case of BS-PT as partly fortuitous. Nevertheless, these results suggest that our approach is adequate.

Figure 2 also shows that the energy reductions associated with the ferroelectric instabilities of BS-PT are considerably larger than those of PZT. In particular, at the MPB we have $\Delta E^{\text{MPB}} = -0.234$ eV for BS-PT and -0.056 eV for PZT. These results are reminiscent of the highly unstable cubic phase of BS previously discussed.

It is tempting to try to connect these numbers with the Curie temperatures of BS-PT and PZT at the MPB. We know that, in principle, the thermal energy required for the system to remain in the high-symmetry paraelectric phase is of the order of $|\Delta E^{\text{MPB}}|$, which suggests that T_C^{MPB} of BS-PT is about 5 times larger than that of PZT, i.e., higher than 1000°C. However, we also know that in systems in which there is competition between different structural instabilities, such an argument can grossly overestimate the transition temperature. In PZT, for example, it is known that there is a competition between the ferroelectric rhombohedral (FE-rho) phase and an antiferrodistortive (AFD) phase involving rotations of the oxygen octahedra.¹⁷ Such a competition also exists in BS-PT, since we find that this material presents a strong AFD instability. Taking PZT as a reference, one could try to estimate the effect of this competition in BS-PT in the following way. The AFD phase supposes a strain of the high-symmetry structure that is opposite to that of the FE-rho phase. At $x=0.5$ for BS-PT the volume per 5-atom cell of the FE-rho phase at the MPB is 415 a.u., while it is 396 a.u. for the AFD phase, resulting in a volume ratio of 1.05. This ratio is 1.01 in PZT, which suggests that the FE-rho–AFD competition will be stronger in BS-PT than in PZT. Energetically, though, we find the opposite trend. The FE-rho phase is more favorable

by 0.15 eV in the case of BS-PT, while in PZT FE-rho is preferred to AFD by only 0.02 eV. Hence, we are unable to determine in which of the two systems the reduction of T_C^{MPB} caused by the FE-rho–AFD competition should be larger. On the other hand, there is another mechanism missed by the VCA and which could significantly lower the transition temperatures of BS-PT. Because BS-PT is a disordered *heterovalent* alloy, internal electric fields will be present in it. Such fields will cause local frustrations and enhance competition between different polarization directions, resulting in a decrease of T_C .^{18,19} In *isovalent* PZT the internal fields and their effects are bound to be much smaller. Quantifying these effects would require a full statistical-mechanics study of the disordered alloys, but that is beyond the scope of this work. In conclusion, all we can say about the issue of the transition temperatures is that our results indicate that T_C^{MPB} of BS-PT could well be significantly larger than that of PZT.

Let us now discuss the structural and polarization data. The ionic and strain relaxations of BS-PT are much larger than those of PZT (see Tables I and II). Importantly, at the MPB composition we find $c/a = 1.079$ and $P_{\text{tet}} = 0.875$ C/m² for BS-PT, to be compared, respectively, with 1.027 and 0.687 C/m² obtained for PZT. The very large values calculated for BS-PT in the MPB region suggest that its piezoelectric response could be very large too, assuming the usual picture in which this arises from easy polarization rotation associated with the near-degeneracy between tetragonal and rhombohedral phases.^{20,21} In fact, according to our results, it would not be surprising to find that BS-PT has even better piezoelectric properties than PZT.

Here we have to note that, while our results for PZT are in reasonable agreement with experiment (at the MPB, c/a and P of PZT are measured to be about 1.025 and 0.75 C/m², respectively^{22,23}), our results for BS-PT significantly deviate from experimental values. Ref. 4 reports $c/a \approx 1.023$ and $P_{\text{tet}} \approx 0.32$ C/m² at the MPB of BS-PT, values that are much smaller than those that result from our VCA calculations. In view of this discrepancy, we decided to assess the reliability of the VCA by studying a 10-atom supercell of BS-PT at 50/50 composition. We have chosen an fcc supercell in which there is rocksalt ordering both on the A sublattice (Bi/Pb) and on the B sublattice (Sc/Ti). The resulting supercell has T_d symmetry, so that all tetragonal ferroelectric domain orientations remain degenerate, while the rhombohedral domains split in two groups of four degenerate orientations. (Here we report results for the lower-energy rhombohedral domains only.) The results, summarized in Table I, display a significant reduction in the c/a of the tetragonal phase, but not large enough to reconcile theory with experiment. The VCA error is presumably maximum at $x = 0.5$, so at x_{MPB} we would expect that c/a should be at least 1.045, still significantly larger than the experimental value. Regarding the polarization, the 10-atom supercell values are actually larger than the VCA results.

In Table I we also included results corresponding to the analogous 10-atom supercell calculations for PZT. As expected,¹⁰ the VCA is more accurate for PZT (isovalent alloy) than for BS-PT (heterovalent). This is further confirmed by the atomic relaxation data (not shown here).

Hence, for BS-PT a relatively large discrepancy between theory and experiment remains. Its origins are most probably related to the differences between the idealized crystalline samples we consider and the ceramic samples actually grown (the internal fields present in real disordered samples are likely to play a particularly relevant role). In any case, we hope that the very large c/a and polarizations we obtain at the MPB will stimulate further experimental study of this promising system.²⁴

V. ALLOYS: PIEZOELECTRIC RESPONSE NEAR THE MPB

Finally, we compute the piezoelectric response of BS-PT, and compare with that of PZT. First we investigate the coefficients $e_{ij} = dP_i/d\eta_j$ that describe the so-called *inverse* piezoelectric effect (η_j is the j -th component of the strain tensor in Voigt notation).²⁶ We report here our results for e_{15} of the tetragonal phase, the coefficient known to be responsible for the large piezoelectric response of PZT.^{21,27} We focus on VCA alloys close to the MPB on the tetragonal side; specifically, we consider BS-PT at $x = 0.7$ (BS-PT $^{x=0.7}$) and PZT at $x = 0.6$ (PZT $^{x=0.6}$).

Following Ref. 28, we split the piezoelectric coefficient into two parts

$$e_{15} = e_{15,i} + e_{15,c}, \quad (2)$$

where $e_{15,c}$ is computed at fixed internal atomic coordinates (“clamped-ion” term) and

$$e_{15,i} = \sum_s \frac{ea}{v} Z_{11}^*(s) \frac{du_1(s)}{d\eta_5}, \quad (3)$$

(“internal-strain” term). Here s runs over the atoms in the unit cell, e is the magnitude of the electron charge, Z_{11}^* is the effective charge associated with displacements u_1 along the x direction, a is the lattice constant in the x direction, and v is the unit cell volume.

For BS-PT $^{x=0.7}$ we obtain $e_{15,c} = -0.93$ C/m² and $e_{15,i} = 8.18$ C/m², which add up to $e_{15} = 7.25$ C/m². For PZT $^{x=0.6}$ we obtain $e_{15,c} = -0.66$ C/m², $e_{15,i} = 8.24$ C/m², and $e_{15} = 7.58$ C/m². Hence, both systems have a similar e_{15} , and in both the internal-strain contribution strongly dominates the response. To understand this, we note that a large value of $e_{15,i}$ can arise in Eq. (3) either from a “dielectric effect” (large Z^*) or an “elastic effect” (large response of the internal coordinates to strain, i.e., large $du_1/d\eta_5$). Table III shows the calculated values of Z_{11}^* and $du_1/d\eta_5$ for all atoms in the

TABLE III. Effective charges Z_{11}^* and derivatives $du_1/d\eta_5$ associated with the $e_{15,i}$ piezoelectric coefficients of VCA BS-PT $^{x=0.7}$ and PZT $^{x=0.6}$. Derivatives given in units of a , the lattice parameter along the x direction; $a=7.27$ a.u. for BS-PT $^{x=0.7}$ and $a=7.42$ a.u. for PZT $^{x=0.6}$. We use the convention that $\sum_s du_1(s)/d\eta_5 = 0$.

	Z_{11}^*		$du_1/d\eta_5$	
	BS-PT $^{x=0.7}$	PZT $^{x=0.6}$	BS-PT $^{x=0.7}$	PZT $^{x=0.6}$
A	4.26	3.82	1.00	0.92
B	5.27	6.64	0.07	0.16
O $_x$	-4.47	-5.23	0.09	0.07
O $_y$	-2.77	-2.90	-0.41	-0.51
O $_z$	-2.29	-2.33	-0.76	-0.64

unit cell of VCA BS-PT $^{x=0.7}$ and PZT $^{x=0.6}$. In both systems the response is mainly associated with an enhanced covalent bonding between the A ion and oxygens O $_y$ and O $_z$, as pictorially shown in Fig. 3. Our results further suggest that the substitution of Pb by Bi enhances such a mechanism, consistent with the fact that Bi is more electronegative than Pb. The B ion contributes by shifting closer to O $_x$, but for the B–O $_x$ pair the elastic effect is substantially smaller than it is in the case of A–O $_y$ and A–O $_z$. We also note that when these results are compared with the analogous ones for the smaller e_{33} coefficient (not shown here – see Refs. 10 and 28 for related PZT results), one finds that it is the elastic effect that makes e_{15} particularly large.

The above results on e_{15} have revealed much about the chemical origin of the piezoelectric response of these systems. However, the energetics of the piezoelectric response, as well as the actual technological interest of a material, is best characterized by the *direct* piezoelectric coefficients $d_{ij} = dP_i/d\sigma_j$ reflecting the polarization that develops in direction i by application of a *stress* with Voigt component j (or equivalently, the strain j induced by an electric field along i). In particular, d_{15} measures the ease of polarization rotation associated with the large responses at the MPB. Technical difficulties have traditionally hampered the direct calculation of d_{ij} coefficients from first principles.²⁹ In the present case, however, it is not hard to show that d_{15} is just given by e_{15}/\tilde{C}_5 , where \tilde{C}_5 is the shear elastic constant associated with η_5 when the atomic positions are allowed to relax in response to the strain (i.e., the *dressed* elastic constant) at fixed electric field. We calculated $d_{15} = 168$ pC/N (with $\tilde{C}_5 = 0.62$ a.u.) for BS-PT $^{x=0.7}$ and $d_{15} = 196$ pC/N (with $\tilde{C}_5 = 0.56$ a.u.) for PZT $^{x=0.6}$. These results agree in magnitude with the piezoelectric coefficients of ceramic samples of BS-PT and PZT measured at room temperature and at the MPB, as well as with the semiempirical calculation of Wu and Krakauer for an ordered PZT supercell.²⁷

Thus, our calculations clearly provide evidence that BS-PT can be expected to be a piezoelectric of com-

parable quality to PZT. This conclusion, as well as the leading role of Bi and/or Pb in the response, is further supported by calculations of e_{33} in the tetragonal phase of the above-mentioned 10-atom supercells (i.e., by calculations in which the VCA was not used).

VI. SUMMARY AND CONCLUSIONS

Our first-principles study of BS-PT indicates that this material displays very large structural distortions and polarizations at the MPB. In particular, we obtain c/a between 1.05 and 1.08 and $P_{\text{tet}} \approx 0.9 \text{ C/m}^2$. We also find that the piezoelectric response of BS-PT near the MPB is comparable to that of PZT.

Our calculations show that the large polarization and piezoelectric responses in BS-PT are mainly related with the onset of Bi/Pb- $6p$ -O- $2p$ hybridization, a mechanism that is enhanced upon substitution of Pb by Bi, since Bi is a more covalent atom. Our results also provide evidence of the dominant role of Pb in the piezoelectric response of PZT, in agreement with recent experimental studies.⁷ In both BS-PT and PZT, this predominance of the A-site ions is related to a large elastic effect, i.e., a large displacement of the ions in response to strain.

Our results are in reasonably good agreement with experiment. The quantitative discrepancies between theory and experiment (in particular, for the values of c/a and the polarizations at the MPB) suggest that the intrinsic piezoelectric properties of BS-PT alloys may be even better than those measured experimentally to date. We thus hope that our results will stimulate further experimental work on this and related materials systems.

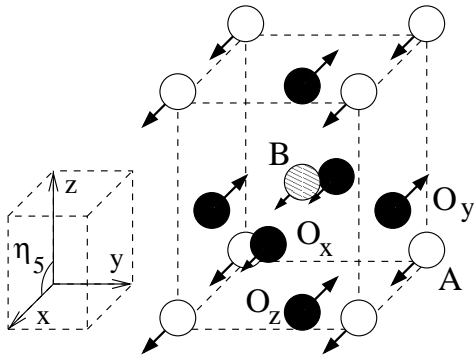


FIG. 3. Sketch of the unit cell of the tetragonal phase of VCA BS-PT or PZT. The arrows represent the displacements associated with $e_{15} = dP_1/d\eta_5$. Atoms in the pairs A- O_y , A- O_z , and B- O_x approach each other.

ACKNOWLEDGMENTS

J. I. thanks J. B. Neaton for many stimulating discussions. This work was supported by ONR Grant No. N0014-97-1-0048 and by the Center for Piezoelectrics by Design (CPD) under ONR Grant N00014-01-1-0365. Computational facilities for the work were also provided by the CPD.

- ¹ K. Uchino, *Piezoelectric Actuators and Ultrasonic Motors* (Kluwer Academic Publishers, Boston, 1996).
- ² S.-E. Park and W. Hackenberger, *Curr. Opin. Solid State Mater. Sci.* **6**, 11 (2002).
- ³ B. Noheda, *Curr. Opin. Solid State Mater. Sci.* **6**, 27 (2002).
- ⁴ R. E. Eitel, C. A. Randall, T. R. Shrout, P. W. Rehrig, W. Hackenberger, and S.-E. Park, *Jap. J. Appl. Phys.* **40**, 5999 (2001); R. E. Eitel, C. A. Randall, T. R. Shrout, and S.-E. Park, *Jap. J. Appl. Phys.* **41**, 1 (2002).
- ⁵ R. E. Cohen, *Nature* **358**, 136 (1992).
- ⁶ M. Posternak, R. Resta, and A. Baldereschi, *Phys. Rev. B* **50**, 8911 (1994).
- ⁷ T. Egami *et al.*, Proceedings of “Fundamental Physics of Ferroelectrics” (Washington DC, 2002), R. E. Cohen, ed. (AIP, Melville, New York, 2002), p. 216.
- ⁸ D. Vanderbilt, *Phys. Rev. B* **41**, 7892 (1990).
- ⁹ R. D. King-Smith and D. Vanderbilt, *Phys. Rev. B* **47**, 1651 (1993).
- ¹⁰ L. Bellaiche and D. Vanderbilt, *Phys. Rev. B* **61**, 7877 (2000).
- ¹¹ N. J. Ramer and A. M. Rappe, *Phys. Rev. B* **62**, 743 (2000).
- ¹² This study could not be accomplished experimentally, since perovskite BS is not stable at ambient pressure.⁴
- ¹³ The atomic relaxations of some of the systems studied here are so large that very large P 's, approaching the “quantum of polarization”,⁹ might be expected. We thus made sure to remain on the correct polarization branch by requiring a smooth behavior of $P(x)$. However, the reported polarizations turned out to remain small enough that this problem did not really arise (e.g., compare with $2e/a^2 \simeq 2.3 \text{ C/m}^2$ for tetragonal BS).
- ¹⁴ See band structures for a family of ferroelectric perovskites in Fig. 4 of R. D. King-Smith and D. Vanderbilt, *Phys. Rev. B* **49**, 5828 (1994). Note that PZ is the only material with a band structure similar to that of BS.
- ¹⁵ A significant Bi- $6p$ -O- $2p$ hybridization was also found in the magnetic perovskite BiMnO₃. See N.A. Hill and K.M. Rabe, *Phys. Rev. B* **49**, 8759 (1999).
- ¹⁶ The ionic radii used in this article were taken from R. D. Shannon, *Acta Cryst. A* **32**, 751 (1976).
- ¹⁷ M. Fornari and D. J. Singh, *Phys. Rev. B* **63**, 092101 (2001).
- ¹⁸ J. Íñiguez and L. Bellaiche, *Phys. Rev. Lett.* **87**, 095503 (2001).
- ¹⁹ A. M. George, J. Íñiguez, and L. Bellaiche, *Nature* **413**, 54

- (2001).
- ²⁰ H. Fu and R. E. Cohen, *Nature* **403**, 281 (2000).
- ²¹ L. Bellaiche, A. García, and D. Vanderbilt, *Phys. Rev. Lett.* **84**, 5427 (2000).
- ²² B. Noheda, D. E. Cox, G. Shirane, J. A. Gonzalo, L. E. Cross, and S.-E. Park, *Appl. Phys. Lett.* **74**, 2059 (1999).
- ²³ D. Berlincourt and H. H. A. Krueger, *J. Appl. Phys.* **30**, 1804 (1959).
- ²⁴ Ref. 4 reports that, as the PT limit is approached from the MPB side, P_{tet} decreases as c/a increases, which is a very unusual behavior (P_{tet} is found to grow with c/a in all systems we are aware of). Also, P_{tet} should reach a value of approximately 0.75 C/m^2 in the PT limit,²⁵ which seems inconsistent with the results of Ref. 4.
- ²⁵ M. E. Lines and A. M. Glass, *Principles and Applications of Ferroelectrics and Related Materials* (Clarendon Press, Oxford, 1977).
- ²⁶ Here we discuss the *proper* piezoelectric response, which we calculate as in D. Vanderbilt, *J. Phys. Chem. Sol.* **61**, 147 (2000).
- ²⁷ Z. Wu and H. Krakauer, Proceedings of “Fundamental Physics of Ferroelectrics” (Washington DC, 2002), R. E. Cohen, ed. (AIP, Melville, New York, 2002), p. 9.
- ²⁸ L. Bellaiche and D. Vanderbilt, *Phys. Rev. Lett.* **83**, 1347 (1999).
- ²⁹ The only direct first-principles calculation of d_{ij} coefficients that we are aware of is the recent one of F. Bernardini and V. Fiorentini [*Appl. Phys. Lett.* **80**, 4145 (2002)] who used a damped Parrinello-Rahman dynamics to study III-V nitrides under applied stress.